POLISH ACADEMY OF SCIENCES - COMMITTEE OF MATERIALS SCIENCE
SILESIAN UNIVERSITY OF TECHNOLOGY OF GLIWICE
INSTITUTE OF ENGINEERING MATERIALS AND BIOMATERIALS
ASSOCIATION OF ALUMNI OF SILESIAN UNIVERSITY OF TECHNOLOGY
Conference Proceedings
12th INTERNATIONAL SCIENTIFIC CONFERENCE
ACHIEVEMENTS IN MECHANICAL & MATERIALS ENGINEERING

Prediction of mechanical properties and microstructure distribution of quenched and tempered steel shaft

B. Smoljan

Faculty of Engineering, Chair of Material Science and Engineering,
Vukovarska 58, 51000 Rijeka, Croatia

An investigation of modeling of the quenching of steel workpiece of complex form has done. An algorithm of computer simulation of transient temperature fields is based on finite volume method.

Heat transfer coefficient and heat conductivity coefficient values involved in mathematical model have been obtained by the inversion method, i.e., by the calibration.

An algorithm for prediction of specimen hardness is based on *Jominy* test results. Hardness in specimen points was calculated by the conversion of calculated characteristic cooling time for phase transformation $t_{8/5}$ to hardness. Mechanical properties are predicted based on calculated hardness.

The inversion method of phase portion estimation based on calculated hardness in the quenched steel has been established.

The designed method has been used in computer simulation of phase portion and mechanical properties in quenched specimens of steel 41 Cr 4 (DIN).

1. INTRODUCTION

Steel quenching could be defined as "cooling of steel workpieces at a rate faster than still air" [1]. The cooling rate has to be so fast that austenite mainly will be transformed within martensite and bainite ranges.

Simulation of steel quenching is a complex problem, dealing with estimation of mechanical properties and microstructure, and dealing with evaluation of residual stresses and distortions after the quenching.

Research of numerical simulation of hardening degree, i.e. hardness and microstructure distribution in quenched steel specimen is one of with high priority research in simulation of phenomena of steel quenching [2].

Simulation of phase transformation is in the root of the simulation steel quenching. A model of quenching would not be considered representative of the actual process if it does not incorporate the effects of phase transformations. Phase transformation modeling is one of the main challenges in modeling of heat treatment [1].

Simulation of anyone process can be made successfully only if all mechanisms of process are well known and if the appropriate mathematical methods are used. Unfortunately the mechanism of phase transformations is not fully understood and interactive influence of different elements, austenitizing temperature, etc. usually are not taken in account. The errors

in phase transformation calculation could be extremely great if a model is based only on grain size of prior austenite, austenitizing temperature and elemental composition of steel. Phase transformation kinetic depends also on the degree of solution of the carbides and it cannot be accurately predicted only from elemental composition. The grain size at the austenitizing temperature must be known in calculation of phase transformation kinetic. Moreover, in practice numerous phase transformation calculations are based just on statistic correlation between chemical composition and final microstructure as result of quenching.

The investigations of steel quenching suggests that choosing a proper representative of the cooling phenomenon, which is relevant for structural transformation is one of the most important factor for a good simulation of hardening [3] [4].

2. NUMERICAL SIMULATION OF SPECIMEN COOLING

Transient temperature field in an isotropic rigid body can be defined by 2-D final volume formulation. The control volume for a 2-D situation is shown in Figure 1.

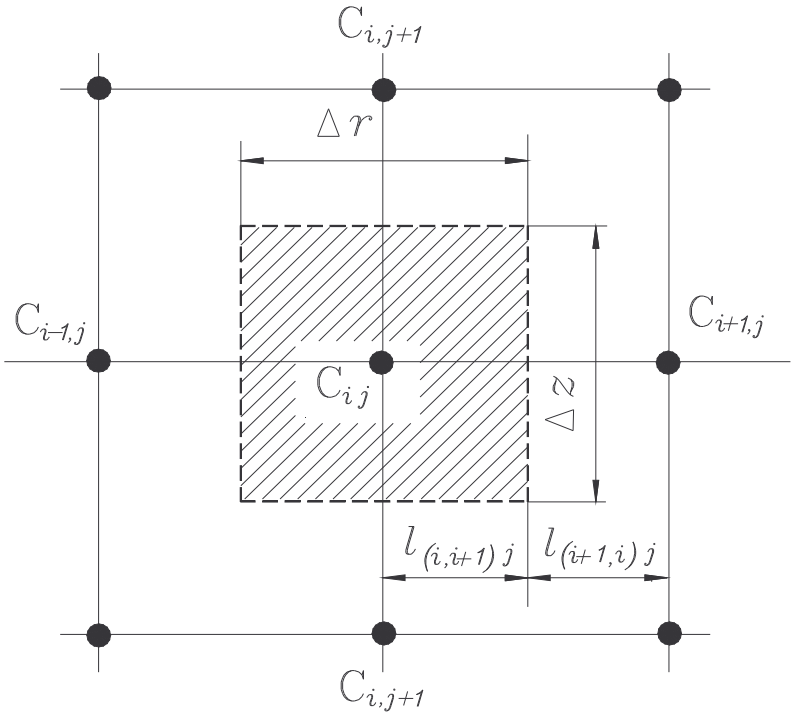

Figure 1. Control volume for 2-D situation

Discretization equations by finite volume method formulation, i.e., algebraic equation system is equal [5][6]:

$$T_{ij}^{l}\left(\sum_{m=1}^{2} b_{(i,i+n)j}+\sum_{m=1}^{2} b_{i(j,j+n)}+b_{ij}\right)=\sum_{m=1}^{2}\left(b_{(i,i+n)j}T_{(i,i+n)j}^{l}+b_{i(j,j+n)}T_{i(j,j+n)}^{l}\right)+b_{ij}T_{ij}^{0}$$

$$i=1,2\ldots i_{\max};\ j=1,2\ldots j_{\max} \qquad (1)$$

$$n=3-2m$$

In equation (1) $b_{ij} = (\rho_{ij}\ c_{ij}\ \Delta V_{ij})/\Delta t$; $b_{(i,i+n)j} = W_{(i,i+n)j}^{-1}$ and $b_{i(j,j+n)} = W_{i(j,j+n)}^{-1}$. Variable $W_{(i,i+n)j}$ is the thermal resistance between ij and $i+n,j$ volume and variable $W_{i(j,j+n)}$ is the thermal resistance between ij and $i,j+n$ volume ($n=\pm 1$):

$$W_{(i,i+n)j} = \frac{1}{\Delta F_{(i,i+n)j}} \left(\frac{l_{(i,i+n)j}}{\lambda_{ij}} + \frac{l_{(i+n,i)j}}{\lambda_{i+n,j}} \right) \tag{2}$$

$$W_{i(j,j+n)} = \frac{1}{\Delta F_{i(j,j+n)}} \left(\frac{l_{i(j,j+n)}}{\lambda_{ij}} + \frac{l_{i(j+n,j)}}{\lambda_{j+n,j}} \right) \tag{3}$$

Thermal resistances for boundary volume are:

$$W_{(i,i+n)j} = \frac{1}{\Delta F_{(i,i+n)j}} \left(\frac{l_{(i,i+n)j}}{\lambda_{ij}} + \frac{1}{\alpha_{Ts_{(i,i+n)j}} \cos\varphi_{r(i,i+n)j}} \right) \tag{4}$$

$$W_{i(j,j+n)} = \frac{1}{\Delta F_{i(j,j+n)}} \left(\frac{l_{i(j,j+n)}}{\lambda_{ij}} + \frac{1}{\alpha_{Ts_{i(j,j+n)}} \cos\varphi_{z\,i(j,j+n)}} \right) \tag{5}$$

were λ is heat conduction coefficient $Wm^{-1}K^{-1}$, ρ is density in kgm^{-3}, and c is specific heat capacity in $Jkg^{-1}\ K^{-1}$ and α is heat transfer coefficient in $Wm^{-2}K^{-1}$, α_{Ts} is coefficient of heat transfer at the boundary temperature which is equal to T_s.

Solution of temperature field change is determined by solution of discretization system for any time step Δt. Time of cooling from T_a to some temperature in particular grid point is determined by the summation of steps Δt_m.

$$t_{ij} = \sum_{m=1}^{M} \Delta t_m \tag{6}$$

In this way the cooling curve, i.e., time - temperature couples ($t_{i,j}$,$T_{i,j}$) in each one grid-point of the specimen can be predicted.

3. MATERIAL DATA INVOLVED IN MATHEMATICAL MODEL OF TRANSIENT TEMPERATURE FIELD

In the transient temperature simulation field is determined by specific heat capacity (c), density (ρ), heat conduction coefficient (λ) and heat transfer coefficient α have to be known.

Heat transfer data can be experimental evaluated or they can be predicted by inverse method, i.e. by calibrating [7][8].

Surface heat transfer coefficient evaluation is the most difficult of the evaluation physical properties used in the mathematical modeling of steel quenching. First, magnitude of heat transfer coefficient remarkable depends on surface temperature and variations of the conditions in the quenching bath and the state of a specimen surface. Specimen shape and size also affect heat transfer coefficient. In quenching, it is a rule that different locations in a specimen have different values of heat transfer coefficient.

Variable ρ for steel is equal ~7800 kgm^{-3} and accepted values of variable *c* are shown in Table 1.

Table 1.
Accepted specific heat capacity of steel

Temperature, ϑ/°C	0	100	250	370	500	700	760	1000	Transformation
Specific heat capacity/ $Jkg^{-1}K^{-1}$	30.6	22.5	19.8	18.0	16.5	16.5	17.1	18.0	Austenite to martensite
	30.6	26.1	21.6	18.0	16.5	16.5	17.1	18.0	Austenite to (bainite +martensite), or bainite
	30.6	28.8	25.2	21.6	16.7	16.5	17.1	18.0	Austenite to (pearlite + bainite), or pearlite

Using the *Crafts -Lamont* diagrams optimization procedure for calibration of heat conduction coefficient (λ) and heat transfer coefficient (α) was done [8]. By varying both, values of heat transfer coefficient and heat conduction coefficient the calibration was provided. The time $t_{8/5}$ distribution in cylindrical quenched steel specimen was predicted by the computer simulation. Time $t_{8/5}$ vas calculated for large spectra of a specimen bar diameter ($D=2R$) at position of cylindrical specimens equal to r/R=0, r/R=0.5 and r/R=0.9.

Corresponding *distance* from water - cooled end of *Jominy* specimen to time of cooling $t_{8/5}$ was predicted by the diagram shown in figure 2. The optimal values of both heat transfer and heat conduction coefficients have been estimated by the comparison of estimated distance from water - cooled end of *Jominy* specimen predicted by computer simulation and by *Crafts-Lamont* diagrams. Values of λ and α were accepted when relative differences between distance from water-quenched end estimated by computer simulation and by *Crafts -Lamont* diagrams were negligible. Accepted values of λ are presented in Table 2.

Table 2.
Calibrated values of heat conductivity coefficient of carbon and low alloyed steel

Temperature, ϑ/°C	0	100	250	370	500	700	760	1000	Transformation
Heat conduction coefficient, λ / $Wm^{-1}K^{-1}$	30.6	22.5	19.8	18.0	16.5	16.5	17.1	18.0	Austenite to martensite
	30.6	26.1	21.6	18.0	16.5	16.5	17.1	18.0	Austenite to (bainite +martensite), or bainite
	30.6	28.8	25.2	21.6	16.7	16.5	17.1	18.0	Austenite to (pearlite + bainite), or pearlite

Calibrated values of heat transfer coefficient (α) of water with severity of quenching, i.e., *Grossman's* to H-value equal 1.4 vs. surface temperature is shown in Table 3.

Table 3. Calibrated values of heat transfer coefficient vs. surface temperature for quenching medium with severity of quenching H=0.45

Temperature ϑ / °C	0	360	440	580	900
Heat transfer coefficient α / $Wm^{-1}K^{-1}$	610	800	2830	790	610

4. PREDICTION OF HARDNESS AND MICROSTRUCTURE DISTRIBUTION PHASE PORTION

One of the most important factors for efficient simulation of hardening is the good selection of representative of the cooling phenomena that is relevant for phase transformation [8]. Characteristic cooling time, relevant for phase transformation in most structural steels is the time of cooling from 800 to 500 °C (time $t_{8/5}$) [4]. Everyone location of *Jominy*-specimen and simulated specimen has one characteristic time $t_{8/5}$ [4]. The diagram of distance from the quenched end of *Jomini*-specimen (*Jominy*-distance) vs. cooling time $t_{8/5}$ is shown in Figure 2. The hardness at grid-points can be estimated by the conversion of cooling time $t_{8/5}$ results to hardness by using both, the relation between cooling time and distance from the quenched end of *Jominy* specimen and the *Jominy* hardenability curve.

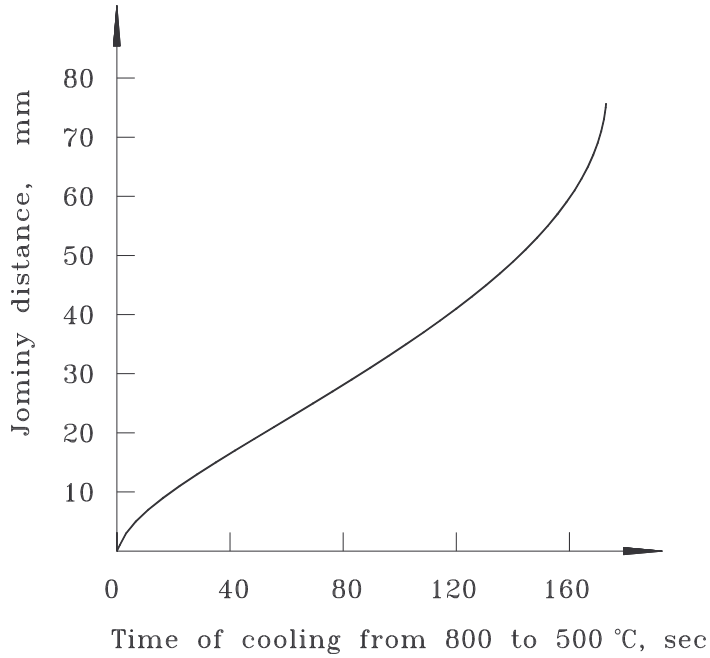

Figure 2. Distance from the quenched end of *Jominy*-specimen vs. cooling time from 800 to 500 °C

Mechanical properties of quenched steel, and also quenched and tempered steel, directly depend on degree of quenched steel hardening [10]. Relation between hardness HV and ultimate tensile stress R_m is equal:

$$R_m = 3.3\ \text{HV, Nmm}^{-2} \tag{7}$$

Yield strength $R_{p0.2}$, specific elongation A_5, reduction of area Z, toughness A_u could be estimated from the ultimate tensile stress R_m or hardness HV [6]:

$$R_e = R_{p0,2} = (0.8+0.1)R_m + 170C - 200,\ \text{Nmm}^{-2} \tag{8}$$

$$Z = 96-(0.062-0.029C)R_m, \quad \% \tag{9}$$

$$A_5 = 46-(0.04-0-012C)R_m, \quad \% \tag{10}$$

$$A_u = 460-(0.59-0.29C)R_m, \quad \text{J} \tag{11}$$

were C is a ratio between the actual hardness and martensite hardness in HRC.

Structure composition of steel cooling depends of actual steel hardness. It can be written that the steel hardness generally is equal:

$$\text{HV} = ((\%\ \text{ferrite})\text{HV}_{(F)} + (\%\ \text{pearlite})\text{HV}_{(P)} + (\%\ \text{bainite})\text{HV}_{(B)} + (\%\ \text{martensite})\text{HV}_{(M)})/100 \tag{12}$$

Amount of phases portion is equal unity:

$$((\%\ \text{ferrite} + \%\ \text{pearlite}) + \%\ \text{bainite} + \%\ \text{martensite}) / 100 = 1 \tag{13}$$

By the equations (12) and (13) is not difficult to predict phase fractions if the hardness (*HV*) of cooling microstructure is known and hardness of microstructure constituents separately is known. Results of austenite decomposition are depending on the chemical composition of steel, severity of cooling, austenitizing temperature and steel history. The austenite decomposition results can be estimated based on time, relevant for structure transformation. The characteristic cooling time, relevant for structure transformation for most structural steels is the time $t_{8/5}$ (Figure 2) [4].

If other heat treatment parameters are constant, the austenite decomposition results in some location of a cooled specimen will depend only of the time $t_{8/5}$. It could be written for *Jominy* test that phase hardness depends of chemical composition (*CC*) and cooling rate parameter (*CRP*) that corresponds to actual distance (*d*) of J*ominy* specimen quenched end. It was adopted that $CRP = \log t_{8/5}^{d}$.

$$HV_d^M = f_M(CC, CRP) = HV_{max}^M - K_M \log \frac{t_{8/5d}^M}{t_{8/5max}^M}; \tag{14}$$

$$HV_d^B = f_B(CC, CRP) = HV_{max}^B - K_B \log \frac{t_{8/5d}^B}{t_{8/5max}^B}; \tag{15}$$

$$HV_d^{P+F} = f_{P+F}(CC, CRP) = HV_N^{P+F} + K_{P+F} \log \frac{t_{8/5N}^{P+F}}{t_{8/5d}^{P+F}}; \tag{16}$$

where N is normalizing, B_{max} is lower bainite. Characteristic value of *HV*, *K* and $t_{8/5}$ in equations (14), (15) and (16) has to be evaluated based on chemical composition for investigated steel combined by *Jominy* test results.

Hardness of quenched structures with characteristic percentage of martensite can be predicted by using the diagram of hardness at different percentages of martensite vs. carbon content after Hodge and Orehoski [10] and *Jominy* curve, but the influence of chemical composition of steel has to be taken in account.

The regression relations between the cooling time from 800 to 500°C for cooling structures of 100%, 50%, 10% and 0% pearlite are established.

$$\log \frac{t_{8/5}^{100\%(P+F)}}{t_{8/5}^{x\%(P+F)}} = f\left(CC, T_a, t_a\right); \tag{17}$$

where (x) is pearlite contents in microstructure, T_a is austenitizing temperature in K; t_a is austenitizing time in h;

Characteristic *Jominy* distances for characteristic time $t_{8/5}$ is estimated using the relation between cooling time and distance from the quenched end of *Jominy* specimen shown in Figure 2.

5. APPLICATION

The presented mathematical model of steel workpiece quenching has been applied in computer simulation of the mechanical properties and microstructure of a quenched shaft. The shaft is shown in Figure 3.

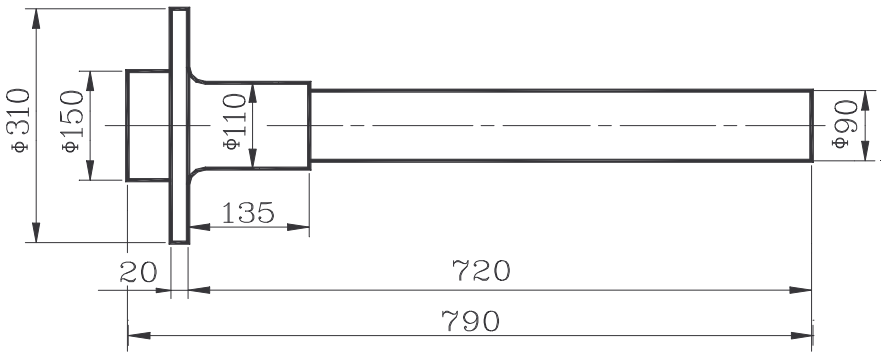

Figure 3. Shaft

The shaft was made of steel 41 Cr 4 (DIN). The *Jominy*-test data of investigated steels are done in Table 4.

Table 4.
Jominy-test data

Distance, mm	1.5	3	5	8	11	15	20	25	30	35	40	80
Hardness HRC	56	55	55	53	52	45	38	35	32	31	30	22

Heat treatment for quenching was heating to 850 ˚C for 30 min and water quenching with slow agitation.

Shaft was quenched in agitated oil with the severity of quenching, i.e., *Grossmann's* H-value equal to 0.45.

The calibrated values of heat transfer coefficient vs. surface temperature of water with severity of quenching H=0.45 are shown in Table 3. Temperature of tempering was equal to 600 ^{o}C.

The phase portion distribution in shaft of steel 41 Cr 4 (DIN) are estimated by computer simulation. Elemental composition of investigated steel was 0.41 % C, 0.28% Si, 0.68% Mn, 1.06 %Cr.

Distribution of properties and microstructure fields of the quenched and tempered shaft is presented in Figure 4.

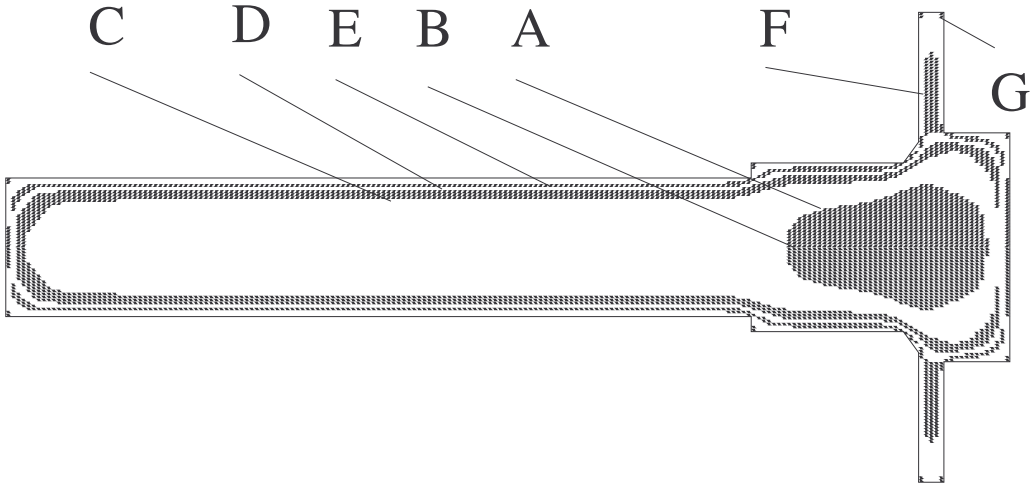

Figure 4. Distribution of properties of quenched shaft of steel 41Cr4

In Table 5 and Table 6 the characteristic values of mechanical properties and microstructures portion are shown.

Table 5.
Predicted properties of the quenched and tempered shaft of steel 41Cr 4

Position	Hardness HRC		R_m Nmm^{-2}	$R_{p0,2}$ Nmm^{-2}	A_5 %	Z %	A_u J
	As-quenched	Quenched and tempered					
A	24	17	683	418	21	59	117
B	28	20	737	476	19	57	101
C	34	23	797	540	18	56	84
D	38	24	818	562	17	55	78
E	44	26.5	861	610	16	54	69
F	48	28	887	639	15	53	65
G	54	32	997	752	12	50	37

When the hardness in quenched specimen points is known and when the phase distribution vs. *Jominy* distances is known it is not difficult to predict the phase distribution in quenched steel specimen (Table 6).

Table 6
Simulated structure composition of quenched shaft

Position	As-quenched hardness HRC	Portion of as-quenched microstructure
A	24	100 % pearlite
B	28	4 % martensite+ 26 % bainite+ 70 % pearlite
C	34	42 % martensite+ 56 % bainite+ 2 % pearlite
D	38	49% martensite + 51% bainite
E	44	71 % martensite + 29 % bainite
F	48	98 % martensite + 2 % bainite
G	54	100 % martensite

6. CONCLUSIONS

A mathematical model of steel quenching has been developed to predict the distribution of mechanical properties in a specimen with complex geometry. The model is based on the finite volume method. The numerical simulation of quenching is consisted of numerical simulation of temperature transient field of cooling process and of numerical simulation of hardening.

The characteristic cooling time, relevant for structure transformation for most structural steels is the time of cooling from 800 to 500 °C (time $t_{8/5}$). The austenite decomposition

results were estimated based on time $t_{8/5}$, relevant for structure transformation. The time $t_{8/5}$ steel specimen was estimated by using the calibrated values of heat transfer coefficient. Hardness in specimen points was estimated on the basis of the time $t_{8/5}$, i.e., by the conversion of mentioned specific time to hardness results. Mechanical properties are calculated based on hardness results.

The inversion method of computer simulation of austenite decomposition and evaluation of quenched phase portion was established. For the calculation of microstructure composition, the hardness in specimen points, *Jominy* test results and chemical composition of steel must be known.

The established mathematical model was applied in computer simulation of microstructure transformation in steel shaft. It can be concluded, that by proposed method mechanical properties and microstructure composition in quenched steel specimen can by successfully calculated.

REFERENCES

1. Theory and Technology of Quenching, eds B. Lišičić, H. Tensi and W. Luty, Springer-Verlag, 1992.
2. E. Just, *Vergüten - Werkstoffbeenflussung durch Härten und Anlassen*, VDI - Bericht, No.256, pp.124-140, 1976.
3. B. Lišćić et al, Workshop Designed System for Quenching Intensity Evaluation and Calculation of Heat Transfer Data, *Proc. of the 1st Inter. Conf. on Quenching & Control of Distortion*, Chicago, Vol. 1, pp. 17-26, 1992.
4. A. Rose et al, Atlas zur Wärmebehandlung der Stähle I, Verlag Stahleisen, Düsseldorf, 1958.
5. S. Patankar, Numerical Heat Transfer and Fluid Flow, McGrawHill Book Company, New York, 1980.
6. B. Smoljan, Numerical Simulation of Steel Quenching, Journal of Materials Engineering and Performance, Vol. 11(1), (2002), pp. 75-80.
7. B. Liščić et al, Workshop Designed System for Quenching Intensity Evaluation and Calculation of Heat Transfer Data, *Proc. of the 1st Inter. Conf. on Quenching & Control of Distortion*, Chicago, Vol. 1, pp. 17-26,1992.
8. B. Smoljan, The Calibration of the Mathematical Model of Steel Quenching, *5th World Seminar on Heat Treatment and Surface Engineering*, Isfahan, Ed. M. Salehi, ISSST and IFHT, Vol. 1, pp. 709-715, 1995.
9. B. Liščić, G. Totten, Controllable Delayed Quenching, Proc. of the Inter. Heat Treating Conf., Schaumburg, pp. 253-262, 1994.
10. S. Hoyt, *Metal Data*, Columbus, Ohio, 1952.